Comparison of precipitable water vapor derived from radiosonde, GPS, and Moderate-Resolution Imaging Spectroradiometer measurements

Zhenhong Li, Jan-Peter Muller, and Paul Cross
Department of Geomatic Engineering, University College London, London, England, UK

Received 2 January 2003; revised 21 July 2003; accepted 1 August 2003; published 29 October 2003.

[1] Atmospheric water vapor is highly variable in both space and time across the Earth, and knowledge of the distribution of water vapor is essential in understanding weather and global climate. In addition, knowledge of the amount of atmospheric water vapor is required for high-precision interferometric synthetic aperture radar (InSAR) applications due to its significant impact on microwave signals, which is the principal motivation for this study. In order to assess the performance of different instruments, i.e., radiosondes (RS), Global Positioning System (GPS), and the Moderate-Resolution Imaging Spectroradiometer (MODIS) and for measuring precipitable water vapor (PWV), coincident observations collected at the Atmospheric Radiation Measurement Southern Great Plains site and at the Herstmonceux site over a 8–11 month period are used for time series intercomparisons. In this study, the Terra MODIS near-infrared water vapor products (Collection 3) were examined. In addition, a first spatial comparison of MODIS PWV and GPS PWV was performed using data covering all of Germany and kindly supplied by the GeoForschungsZentrum Potsdam. Time series comparisons of PWV between radiosondes and GPS show that the scale factors of PWV from radiosondes and GPS agreed to 4% with correlation coefficients higher than 0.98 and standard deviations about 1 mm. A significant day-night difference was found for Vaisala RS90 radiosondes in comparison with GPS PWV, with nighttime launches having a scale factor 4% larger, but agreeing overall better. It is also shown that GPS PWV and RS PWV agreed better with each other than with MODIS PWV, and the differences of MODIS PWV relative to GPS or RS were larger than those between GPS PWV and RS PWV. MODIS PWV appeared to overestimate PWV against RS, with scale factors from 1.14 to 1.20 and standard deviations from 1.6 to 2.2 mm. MODIS PWV appeared to overestimate PWV against GPS, with scale factors from 1.07 to 1.14 and standard deviations varying from 0.8 to 1.4 mm in time series. The larger differences relative to MODIS PWV are likely to be caused by uncertainties in the spectroscopic database for the MODIS retrievals, calibration uncertainties in the radiances measured by MODIS, operational differences of the three systems, and different mapping functions adopted in GPS and MODIS PWV retrievals. We derived a linear fit model to calibrate MODIS PWV, and better agreements between calibrated MODIS PWV and GPS PWV in space have been achieved. This indicates that MODIS PWV products should be updated or calibrated using a linear fit model before being applied to correct InSAR measurements. Also, the potential accuracy of standard resolution (resampled) radiosonde data from the UK Met Office and the University of Wyoming has been assessed. It is demonstrated that some caution needs to be exercised when using standard resolution data. *INDEX TERMS:* 3354 Meteorology and Atmospheric Dynamics: Precipitation (1854); 3360 Meteorology and Atmospheric Dynamics: Remote sensing; 3394 Meteorology and Atmospheric Dynamics: Instruments and techniques; *KEYWORDS:* water vapor, MODIS, GPS

Citation: Li, Z., J.-P. Muller, and P. Cross, Comparison of precipitable water vapor derived from radiosonde, GPS, and Moderate-Resolution Imaging Spectroradiometer measurements, *J. Geophys. Res.*, *108*(D20), 4651, doi:10.1029/2003JD003372, 2003.

0148-0227/03/2003JD003372

1. Introduction

[2] Water vapor is fundamental to the transfer of energy in the atmosphere [*Rocken et al.*, 1997]. It is one of the most important and most abundant greenhouse gases in the

Earth's atmosphere, keeping the temperature of the Earth surface above the freezing level. Atmospheric water vapor plays a key role in the hydrological cycle, which in turn has a fundamental impact on the Earth's climate. The distribution of water vapor varies greatly both in space and time, with values ranging from about 5 cm near the equator to less than one tenth as much at the poles [*Mockler*, 1995]. These changes can lead to sudden changes in local weather (http://www.ae.utexas.edu/courses/ase389p_gps/projects99/whitlock/intro.html). In order to develop accurate weather prediction and global climate models, it is vital to monitor water vapor as accurately as possible.

[3] From a geodetic point of view, tropospheric delay (especially the part due to water vapor) in radio signal propagation is known to be a major source of error for geodetic observations from very long baseline interferometry (VLBI), radar altimetry, Global Positioning System (GPS), and interferometric synthetic aperture radar (InSAR). It is now widely accepted that geodetic observations such as GPS and VLBI present new approaches for the remote sensing of water vapor. In contrast, water vapor is still a major limitation to InSAR, although Interferometric Radar Meteorology (IRM) has been used to study water vapor using the InSAR technique [*Hanssen et al.*, 2001]. For this reason, knowledge of atmospheric water vapor amount is an important requirement for high-precision InSAR applications, which is the principal motivation for this study. *Zebker et al.* [1997] suggested that a 20% spatial or temporal change in relative humidity could result in a 10-cm error in deformation measurement retrievals and up to 100 m of error in derived digital elevation models (DEM) for those interferometric pairs with unfavorable baseline geometries.

[4] Meteorologists have defined several different terms to express the amount of atmospheric water vapor, and one of the most common is precipitable water vapor (PWV). PWV is defined as the total atmospheric water vapor contained in a vertical column of unit cross-sectional area extending between any two specified levels and commonly expressed in terms of the height to which that water substance would stand if completely condensed and collected in a vessel of the same unit cross section [*American Meteorological Society (AMS)*, 2000]. It is also referred to as the total column water vapor [*Ferrare et al.*, 2002]. Currently, measurements of PWV can be obtained in a number of ways, from in situ measurements to remote sensing from satellites [*Mockler*, 1995; *Chaboureau et al.*, 1998]. The objective of this paper is to use PWV retrievals from different instruments to assess their performance through intercomparisons. These instruments are radiosondes (RS), GPS, and the Moderate-Resolution Imaging Spectroradiometer (MODIS).

[5] The radiosonde network has long been the primary in situ observing system for monitoring atmospheric water vapor. Radiosondes provide vertical profiles of meteorological variables such as pressure, temperature, and relative humidity. Sometimes, wind information can be obtained as well. However, the use of radiosondes is restricted by their high operational costs, decreasing sensor performance in cold dry conditions, and their poor coverage over oceans and in the Southern Hemisphere. Usually, radiosondes are expected to produce PWV with an uncertainty of a few millimeters, which is considered to be the accuracy standard of PWV for meteorologists [*Niell et al.*, 2001].

[6] GPS is an increasingly operational tool for measuring precipitable water vapor, which has gained a lot of attention in the meteorological community. GPS signals are delayed when propagating through the troposphere. The total tropospheric delay can be divided into a hydrostatic term, caused primarily by dry gases in the atmosphere, and a wet term, caused by the refractivity due to water vapor [*Davis et al.*, 1985]. GPS measurements provide estimates of the total zenith delay (TZD) using mapping functions. The zenith hydrostatic delay (ZHD) can then be calculated, given the local surface pressure. ZHD subtracted from TZD yields the zenith wet delay (ZWD) from which PWV can be inferred [*Bevis et al.*, 1992]. The primary advantage of GPS is that it makes continuous measurements possible. Furthermore, the spatial density of the current Continuous GPS (CGPS) network is much higher than that of the radiosonde network, and its capital and operational costs are much lower than for RS. The potential for GPS to detect PWV has been well demonstrated [*Emardson et al.*, 1998; *Niell et al.*, 2001]. Agreements at the level of 1–2 mm of PWV between GPS, RS, and microwave water vapor radiometers (WVR) have been reported in previous research [*Emardson et al.*, 2000; *Niell et al.*, 2001]. *Williams et al.* [1998] used the Treuhaft and Lanyi (TL) statistical model to assess the effects that the heterogeneous troposphere has on a synthetic aperture radar (SAR) interferogram and claimed that it is feasible to use CGPS estimates of ZWD to reduce atmospheric noise in SAR interferograms. They also found that an average spacing of 10 km is needed for an accuracy of 5 mm when using a kriging spatial interpolator.

[7] Space-based monitoring is the only effective way to assess water vapor distribution on a global basis, and various missions have been implemented to monitor water vapor amount (e.g., Television and Infrared Operational Satellite (TIROS) Operational Vertical Sounder (TOVS), Special Sensor Microwave/Imager (SSM/I), etc.) [*Chaboureau et al.*, 1998; *Randel et al.*, 1996]. More recently, atmospheric water vapor amount has been continuously measured with the two National Aeronautics and Space Administration (NASA) MODIS instruments. The first was launched on 18 December 1999 on board the Terra Platform and the second was launched on 4 May 2002 on board the Aqua platform. The MODIS Near-Infrared Total Water Product (MODIS product, MOD_05) consists of daytime only total column atmospheric water vapor (designated MODIS PWV). The technique implemented for the MODIS water vapor retrievals uses ratios of radiance from water-vapor-absorbing channels centered near 0.905, 0.936, and 0.94 μm with atmospheric window channels at 0.865 and 1.24 μm. MODIS PWV is claimed to be determined with an accuracy of 5–10% [*Gao and Kaufman*, 2003]. Errors will be greater for retrievals from data collected over dark surfaces or under hazy conditions [*Gao and Kaufman*, 2003].

[8] In this paper, descriptions of retrieval techniques for the three instruments to obtain ZWD (for GPS and RS) and PWV are given in section 2. The results of the time series intercomparisons among RS, GPS, and MODIS PWV are described in section 3. In section 4, a first attempt at a spatial comparison over Germany between GPS and MODIS PWV is presented along with a method to calibrate

Table 1. Summary of RS Data Sets

Data Sets	Number of Profiles	Mean Number of Pressure Levels
ARM SGP (36.61°N, 97.49°W), Vaisala VS90 Radiosonde, 2 December 2001 to 1 August 2002		
HRRS	964	2898
UKMO_EL	688	13
UKMO_HF	690	31
UWRS	683	81
HERS (50.90°N, 0.32°E), Vaisala VS80-H Radiosonde, 15 July 2002 to 31 January 2002		
HRRS	280	2404
UKMO_EL	291	14
UKMO_HF	291	59
UWRS	280	101

MODIS PWV using GPS PWV, followed by detailed discussions in section 5. In section 6, the conclusions of this study are summarized.

2. Data Descriptions and Processing Strategy

2.1. Radiosondes

[9] In this study, radiosonde data over the Atmospheric Radiation Measurement (ARM) Southern Great Plains (SGP) and Herstmonceux (HERS) sites were used, and ZWD was calculated with a ray-tracing program developed by J. Davis, T. Herring, and A. Niell of Massachusetts Institute of Technology, Cambridge (MIT). It is assumed that measured pressure, temperature, and dew-point depression were obtained along a strictly vertical ascent [*Niell et al.*, 2001], although observational evidence suggests that RS ascents are rarely strictly vertical because winds are usually present at all altitudes. ZWD was converted into PWV using the surface temperature (see section 2.2).

2.1.1. The ARM SGP and HERS Sites

[10] The ARM SGP site is located in northern Oklahoma (36.61°N, 97.49°W, 317.0 m above mean sea level (AMSL), Table 1), and Vaisala RS90 radiosondes have been launched four times daily since 1 May 2001. RS90 relative humidity resolution is quoted as 1%, reproducibility is quoted as 2%, and repeatability is quoted as 2%, with a 5% uncertainty in soundings (Vaisala, RS90 radiosondes, 2002, available at http://www.vaisala.com/DynaGen_Attachments/Att2749/2749.pdf). The raw data sent from the radiosonde were processed with the standard ground-station software, and quality controlled (i.e., filtered, edited, and interpolated) before being output with 2-s resolution (http://www.arm.gov/docs/instruments/static/bbss.html). The radiosonde data used in this study covered the period from 2 December 2001 to 1 August 2002.

[11] The HERS site is located at 50.90°N, 0.32°E, 50.9 m AMSL (Table 1) in East Sussex, UK. Vaisala RS80-H radiosondes have been launched twice daily at 2315 and 1115 UT since the beginning of December of 2001, and extra launches sometimes occur at 0515 and 1715 UT when greater detail of the atmospheric conditions overhead are needed (J. Jones, private communication, 2003). Measured range and resolution for RS80 relative humilities are the same as for the RS90 but the reproducibility is quoted as <3% (Vaisala, technical information, 2002, available at http://www.vaisala.com/DynaGen_Attachments/Att2743/2743.pdf). A general problem with Vaisala RS80 radiosondes is that they have been found to exhibit a dry bias, which results from contamination of the humidity sensor during storage and leads to the reported relative humidity values being lower than the actual ones [*Liljegren et al.*, 1999; *Wang*, 2002]. Vaisala changed the desiccant type in the package from clay to a mixture of active charcoal and silica gel in September 1998 and also introduced a new type of protective shield over the sensor boom in May 2000 for RS80 radiosondes [*Wang et al.*, 2002]. *Wang* [2002] evaluated the performance of the new sensor boom cover and found that RS80-H radiosondes with a sensor boom cover are free of contamination. Therefore no contamination correction was required but a modeled ground check correction was used to calibrate the radiosonde humidity sensors for the RS data at the HERS site (J. Jones, private communication, 2003). There were 280 high-resolution profiles available at the HERS site in this study for the period from 16 July 2002 to 31 October 2002.

2.1.2. High-Resolution and Standard Resolution Data

[12] Radiosondes usually take measurements at intervals of approximately 2 s. The high-resolution profiles contain all such data. In contrast, the standard resolution profiles only contain measurements resampled from the high-resolution data at particular pressure levels. Different providers apply different criteria to select pressure levels for transmission and archiving. For instance, the UK Met Office (UKMO hereafter) standard resolution radiosonde data contain measurements at the so-called standard and significant pressure levels. The standard pressure levels are 1000, 925, 850, 700, 500, 400, 300, 250, 200, 150, 100, 70, 50, 30, 20, and 10 hPa, and the significant pressure levels are calculated according to UKMO criteria and constitute levels at which significant events occur in the profile (http://badc.nerc.ac.uk/data/radiosglobe/) (e.g., turning points). In contrast, the University of Wyoming standard resolution radiosonde data (UWRS hereafter) comprise some additional levels evaluated with temperature and relative humidity criteria (http://weather.uwyo.edu/upperair/sounding.html).

[13] In order to examine the effect of the radiosonde resolution on ZWD, comparisons among UKMO, UWRS, and the high-resolution radiosonde data (HRRS hereafter) were performed over the ARM SGP and HERS sites. All of these data consist of height profiles of pressure, temperature, and dew point, but their resolutions are different. A summary of the radiosonde data that were employed for the comparisons is given in Table 1.

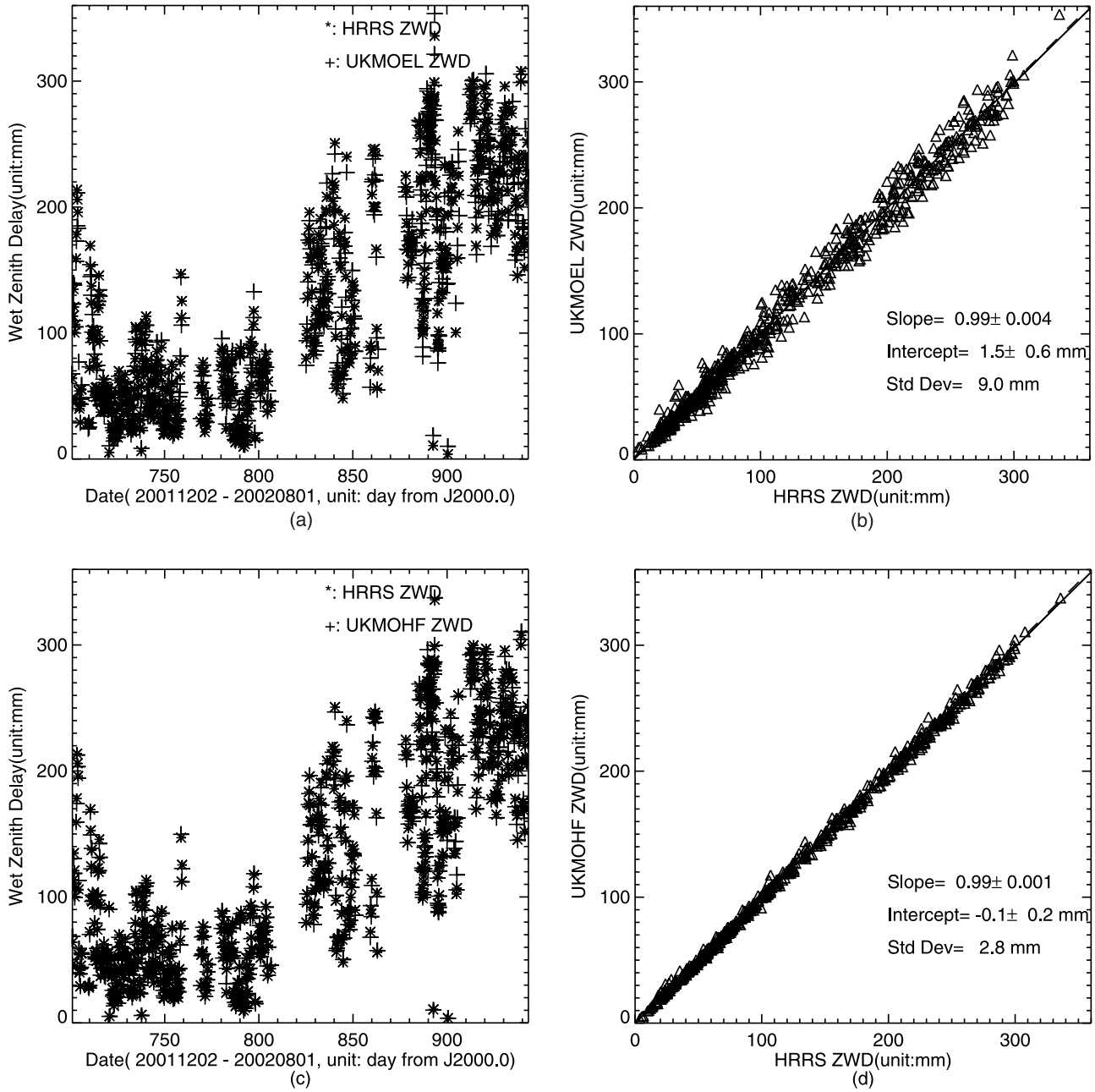

Figure 1. Comparisons between high-resolution radiosonde (HRRS) and UKMO standard resolution radiosonde ZWD estimates above the ARM SGP site during the period from 1 December 2001 to 1 August 2002. Two methods are used to process the UKMO standard resolution data: one is UKMOEL without filling the missing height values in the profiles, the other is UKMOHF with filling in the missing height values using the hypsometric equation (see section 2.1.2). (a) ZWD estimates derived from HRRS and UKMOEL; (b) correlation between HRRS and UKMOEL ZWD estimates; the line of perfect fit (dashed line) and a least squares regression line (solid line) are plotted; (c) ZWD estimates derived from HRRS and UKMOHF; (d) correlation between HRRS and UKMOHF ZWD estimates.

[14] As the UKMO profiles contain heights only at mandatory levels and much higher resolution is given for the meteorological variables [*Mendes et al.*, 2000], two methods were applied to process the UKMO data. The first method eliminated any levels within a sounding that were missing any observation of height, pressure, temperature, or dew point (except for layers above 10 km, where only height, pressure, and temperature were checked because the ray-tracing program employs a model to fill in the missing values) (UKMOEL hereafter). The second method was the same as the first one except that the missing heights were calculated from reported temperature and pressure using the hypsometric equation (UKMOHF hereafter) [*Wright*, 1997; V. Mendes, private communication, 2003] (the former is available at http://www.ofcm.gov/fmh3/text/). In Table 1, it is obvious that UWRS had more levels than the

Table 2. Scale Factors and Zero-Point Offsets for Comparisons of ZWD From Different RS Data Sets

A[a]	B[a]	Number of Samples[b]	a[c]	b, mm[c]	Correlation	Standard Deviation, mm[d]
			ARM SGP			
UKMO_EL	HRRS	624 (39)	0.99 ± 0.004	1.5 ± 0.6	0.99	9.0
UWRS	HRRS	656 (7)	1.00 ± 0.001	−0.7 ± 0.2	1.00	3.1
UKMO_EL	UWRS	647 (23)	1.00 ± 0.005	2.1 ± 0.7	0.99	9.8
UKMO_HF	HRRS	656 (7)	0.99 ± 0.001	−0.1 ± 0.2	1.00	2.8
UKMO_HF	UWRS	644 (26)	1.00 ± 0.000	0.5 ± 0.06	1.00	0.9
			HERS			
UKMO_EL	HRRS	263 (14)	0.94 ± 0.01	9.9 ± 2.0	0.97	8.8
UWRS	HRRS	272 (4)	1.01 ± 0.002	1.1 ± 0.2	1.00	1.0
UKMO_EL	UWRS	262 (13)	0.94 ± 0.01	8.7 ± 2.0	0.97	9.0
UKMO_HF	HRRS	272 (5)	0.99 ± 0.001	−0.1 ± 0.2	1.00	0.9
UKMO_HF	UWRS	255 (20)	0.98 ± 0.001	−1.1 ± 0.2	1.00	0.8

[a]The relation is $A = aB + b$.
[b]Values in brackets in this column refer to those omitted due to the 2σ exclusion.
[c]Uncertainties multiplied by square root(chi-square/(N-2)), where N is the number of samples.
[d]Standard deviation of the linear least squares solutions.

UKMO profiles and UKMOEL had fewer levels than UKMOHF.

[15] The ray-tracing program was used to calculate ZWD from the HRRS, UKMOEL, UKMOHF, and UWRS data over the ARM SGP site. The UKMOEL ZWD was compared to the HRRS ZWD. If the relationship between them was assumed to be linear, i.e., ZWD (UKMOEL) = $a \times$ ZWD (HRRS) + b, a least squares fit gave a scale factor of 0.99 ± 0.004, with an offset at zero of 1.5 ± 0.6 mm (Table 2). The standard deviation was 9.0 mm, with a bias of 0.4 mm. The observations are shown in Figure 1a, and a comparison is shown in Figure 1b. In contrast, a linear fit of the UWRS ZWD to the HRRS ZWD for the same time period yielded a relationship of ZWD (UWRS) = 1.00(± 0.001) × ZWD(HRRS) − 0.7(± 0.2) mm, with a standard deviation of 3.1 mm and a bias of −1.3 mm. Furthermore, a linear fit of the UKMOEL data to the UWRS data had a large standard deviation, 9.8 mm. This means that the UWRS ZWD was in much closer agreement with the HRRS data than the UKMOEL data was. Similar comparison results at the HERS site are also shown in Table 2. As mentioned earlier, there were far fewer pressure levels in the UKMOEL data than in the UWRS data (Table 1). It appeared that the UKMOEL data suffered from an ''aliasing'' artifact, which occurred when the high-resolution data were undersampled.

[16] When the UKMOHF data, i.e., profiles with missing heights filled in, were compared with the HRRS data, the scale factors were close to unity (Figure 1 and Table 2). Standard deviations ranged from 0.9 to 2.8 mm, with biases varying from −0.7 to −1.0 mm. The UKMOHF data were also in good agreement with the UWRS data.

[17] The above comparisons suggest that some caution needs to be exercised when using the standard resolution data, particularly the UKMO data, to validate other data sets.

2.2. GPS

[18] The GPS data were analyzed separately for each UTC day using the GIPSY-OASIS II software package in Precise Point Positioning mode [*Zumberge et al.*, 1997]. Phase measurements were decimated to 300 s in the analysis. The receiver's clock was modeled as a white noise process with updates at each measurement epoch, and ZWD was modeled as a random walk with a σ of 10.2 mm/$\sqrt{h}$. The gradient parameters, G_N and G_E, were modeled as random walk processes with a σ of 0.3 mm/$\sqrt{h}$. Satellite final orbits and clocks were obtained via anonymous FTP (ftp://sideshow.jpl.nasa.gov/pub) from the Jet Propulsion Laboratory (JPL, http://www.jpl.nasa.gov/).

[19] The Niell Mapping Function was used in the processing because of its independence from surface meteorology, small bias, and low seasonal error [*Niell*, 1996; *Niell et al.*, 2001]. Niell et al. evaluated the impacts of the uncertainties of the Niell hydrostatic and wet mapping functions on ZWD. The uncertainty of the hydrostatic mapping function at 5° elevation angle is 1% and results in an uncertainty in the estimated ZWD of about 3 mm (about 0.5 mm of PWV) for the lowest elevation angle 24-hour solutions when the site positions are estimated along with ZWD. For the wet mapping function, the uncertainty at 5° elevation angle is 0.5%. Taking into account the maximum PWV of 50 mm in the study (see section 3), the maximum uncertainty in PWV was 0.25 mm.

[20] On the one hand, there is a loss of sensitivity to ZWD when only high-elevation ray paths are used in the GPS analysis. On the other hand, when low-angle elevation data are included in the analysis, the uncertainty of the mapping function for very low elevation angles along with the noise of the GPS observations due to effects such as multipath and antenna phase center variations increase. A trade-off between the sensitivity of ZWD and the uncertainties of mapping functions and other factors should be made. *MacMillan and Ma* [1994] reported improved VLBI baseline length repeatabilities using an elevation cutoff angle of 7°. *Bar-Sever and Kroger* [1996] found superior agreement in ZWD estimates between a collocated WVR and a GPS receiver using the same cutoff value. Therefore we used an elevation cutoff angle of 7° as a compromise in this study.

[21] Tropospheric delay was estimated in two steps [cf. *Niell et al.*, 2001]. First, the tropospheric delay was deter-

mined together with the site position and receiver's clock. Then the site position was fixed to the average of that day, and only the zenith tropospheric delays and receiver's clocks were estimated. This was done because of the high correlation between height estimates and ZWD estimates, i.e., real variations in ZWD may manifest themselves as apparent variations in height. Therefore retrievals of ZWD will be obtained with less reliability if the height and ZWD are estimated simultaneously.

[22] For the purpose of comparison with MODIS PWV, GPS ZWD needs to be converted into PWV using the following relationship:

$$\mathrm{PWV} = \Pi \times \mathrm{ZWD}, \tag{1}$$

where Π is a dimensionless conversion factor, approximately equal to 6.2. This is dependent on the weighted mean temperature of the atmosphere and can be inferred either from surface temperature measurements or from numerical weather models with an accuracy of about 2% or better [*Bevis et al.*, 1992, 1994; *Quinn and Herring*, 1996; *Mendes et al.*, 2000]. The mean temperature of the atmosphere (T_m) used in this study was determined by $T_m = 70.2 + 0.72T_s$ [*Bevis et al.*, 1992], where T_s is the surface temperature and was obtained from GPS meteorological data.

[23] In this study, the GeoForschungsZentrum, Potsdam (GFZ), near real-time GPS PWV retrievals were also used to compare MODIS PWV temporally and spatially across Germany. The GPS Atmosphere Sounding Project (GASP), led by GFZ, utilizes a dense GPS network with more than 100 sites all over Germany. In contrast to JPL GIPSY, the GFZ near-real-time (NRT) processor, EPOS.P.V2, uses the least squares adjustment instead of Square Root Information Filter (SRIF). The EPOS.P.V2 is used to handle GPS data in two steps. The first step is to estimate high-quality GPS orbits and clocks from a global network with five GASP stations; the second is to estimate zenith total delay with a resolution of 30 min using Precise Point Positioning based on the fixed orbits and clocks. GFZ currently works on a sliding 12-hour data window with a sampling rate of 150 s and an elevation cutoff angle of 7°. For the conversion from ZWD to PWV the physical constants given by *Bevis et al.* [1992] are taken. Comparisons with postprocessed results as well as validation with independent techniques and models showed that an accuracy of better than 2 mm in the precipitable water vapor can be achieved with a standard deviation of better than 1 mm [*Gendt et al.*, 2001; *Reigber et al.*, 2002; Y. Liu, private communication, 2003].

2.3. MODIS Near-Infrared Precipitable Water Vapor Product

[24] The MODIS near-infrared precipitable water vapor properties are generated during the daytime and stored in the MOD05 product [*Gao and Kaufman*, 2003], which includes a cloud mask, geolocation data, and scanning time. The accuracy is currently claimed to be 5–10% [*Gao and Kaufman*, 2003]. *Ferrare et al.* [2002] also reported that MODIS near-infrared PWV agreed well with microwave radiometer (MWR) PWV measurements, with bias and RMS differences generally less than 10%.

[25] The current resolution of the MODIS PWV product is 1×1 km (at nadir), and the output grid of a single Level-2 MODIS granule is 1350 one-km pixels in width and 2030 one-km pixels in length. In this study, the MODIS PWV Collection 3 products from Terra were examined. As MODIS PWV is sensitive to the presence of clouds in the field of view, only MODIS PWV values collected under clear sky conditions were used in this study. The cloud mask product used had to indicate at least 95% confidence clear.

3. Comparisons Among RS, GPS, and MODIS PWV in Time Series

[26] Intercomparisons have been made among all three techniques for time series measurements. Note that all statistics are given after 2σ elimination; that is, all differences more than twice the standard deviation were considered to be outliers and were removed. This elimination was mainly needed when poor collocations between the data in either time or space were found.

[27] As MODIS PWV is sensitive to the presence of clouds and only about 25% of all observations appear to be cloud free at midlatitudes in northern Europe (Z. Li et al., manuscript in preparation, 2003), long data sets are required. Therefore bearing in mind the good agreement between the HRRS and the UKMOHF ZWD, the UKMOHF data were used to compare with GPS and MODIS PWV products at the HERS site for the period from 2 December 2001 to 31 October 2002. The HERS International GPS Service (IGS) station is located at 50.87°N, 0.34°E (76.49 m ellipsoid), 3.8 km away from the HERS radiosonde site. The amount of PWV varied from 0 to 40 mm, with a mean of 17 mm at the site during this period. Meteorological data were also collected at the GPS site in order to convert ZWD into PWV. All GPS observation data were available, but 1-day GPS MET data were missing, and 3-day GPS MET data were incomplete.

[28] For the ARM SGP site, the HRRS data were used in the comparisons during the period from 2 December 2001 to 1 August 2002. The LMNO IGS site is 5.8 km away from the ARM SGP Radiosonde site. The amount of PWV ranged from 0 to 55 mm, with a mean of 19 mm during this period. There were only 147 days of coincident GPS observation and MET data.

3.1. Comparisons Between GPS and RS PWV

[29] The same algorithm was used to convert ZWD into PWV for both GPS and RS data; therefore this conversion does not add any additional uncertainty for the comparisons between GPS and RS PWV. Consistency was expected with the other comparisons, so that PWV instead of ZWD was compared and the GPS PWV values were averaged over 30-min time intervals during the radiosonde launches and flights.

[30] Figure 2 shows PWV from the UKMOHF data for the period from 2 December 2001 to 31 October 2002 compared with retrievals from GPS. There were 931 valid pairs. A high correlation coefficient, 0.99, was observed between the two data sets. GPS PWV was 1.02 ± 0.004 times greater than RS PWV, with a zero-point offset of -0.3 ± 0.06 mm.

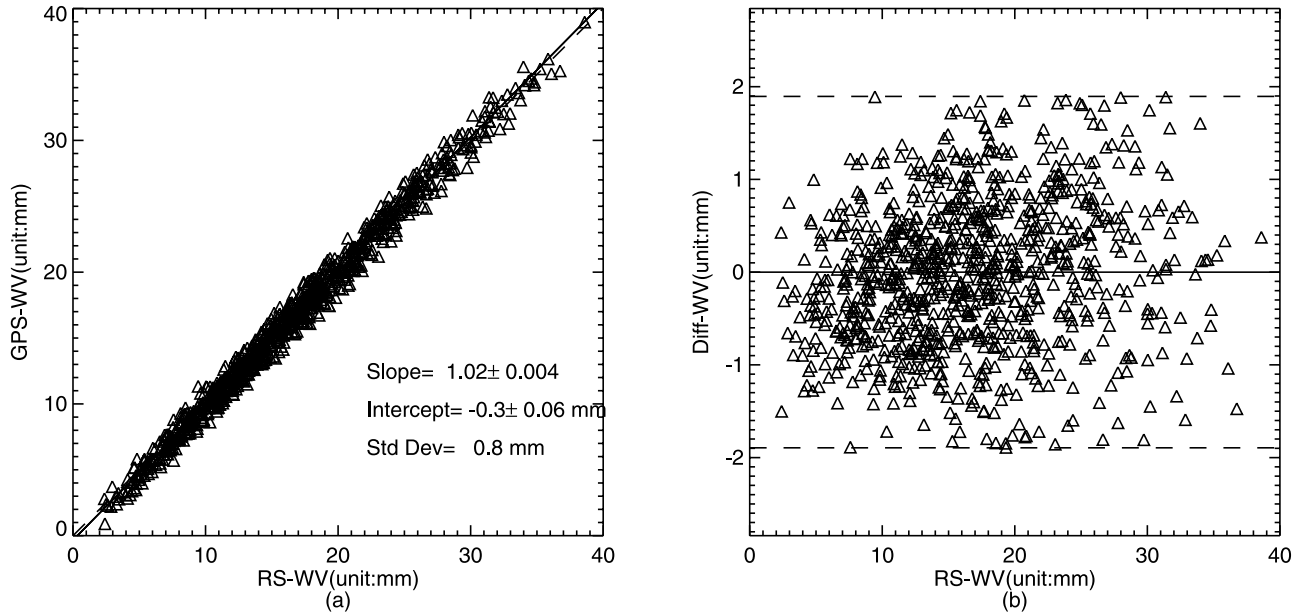

Figure 2. Scatterplots of UKMOHF RS ZWD and GPS ZWD for both daytime and nighttime at the HERS station from 2 December 2001 to 31 October 2002. (a) The line of perfect fit (dashed line) and a least squares regression line (solid line) are plotted. The number of valid samples was 931, and 54 samples were omitted due to the 2σ exclusion; (b) difference in PWV (diff-WV) = GPS PWV − RS PWV. The solid line stands for the zero difference, and the dashed lines stand for the 2σ values.

[31] Some previous studies revealed that there are day-night differences in radiosonde relative humidity measurements [e.g., *Smout et al.*, 2001] (available at http://www.met-office.gov.uk/research/interproj/radiosonde/reports/eurs90u.doc). In order to check the effect of day-night differences, comparisons between GPS PWV and PS PWV were also performed by separating daytime and nighttime cases (Table 3). A linear fit of RS PWV and GPS PWV at the HERS site using only the daytime results yielded the relationship, RS PWV (Day) = 0.96(±0.006) × GPS PWV (Day) + 0.5(±0.1) mm. At nighttime, a linear relationship, RS PWV (Day) = 0.97(±0.004) × GPS PWV (Day) + 0.5(±0.08) mm, was found. The scale factor variation due to day-night differences was ∼1% for RS80 PWV relative to GPS measurements at the HERS site. By comparison, the scale factors for the RS90 PWV relative to GPS PWV measurements changed from 0.97 ± 0.005 in the daytime to 1.01 ± 0.005 at nighttime at the ARM SGP site. A possible cause for the larger scale factor variation at the ARM SGP site is that the RS90 sensors were heated by the sun's solar radiation during the day, which resulted in lower relative humidity measurements, while there is a cap on the RS80 sensors [*Smout et al.*, 2001].

[32] As the MODIS near-infrared water vapor retrieval algorithm relies on observations of water vapor attenuation of near-IR solar radiation reflected by surfaces and clouds, the product is produced only in the daytime [*Gao and Kaufman*, 2003]. For consistency purposes, only daytime measurements were used in Table 4. The mean and standard

Table 3. Day-Night Differences of the Comparisons Between GPS PWV and RS PWV

Time	Sample Number	*A*	*b*, mm	Standard Deviation, mm[a]	Correlation Coefficient
		HERS (RS80-H)[b]			
All time	931	0.97 ± 0.003	0.5 ± 0.06	0.8	0.99
Daytime	411	0.96 ± 0.006	0.5 ± 0.1	0.8	0.99
Nighttime	517	0.97 ± 0.004	0.5 ± 0.08	0.7	0.99
		ARM SGP (RS90)[b]			
All time	508	0.99 ± 0.004	1.1 ± 0.1	1.2	0.99
Daytime	263	0.97 ± 0.005	1.0 ± 0.1	1.2	0.99
Nighttime	245	1.01 ± 0.005	1.1 ± 0.1	1.0	1.00

[a]Standard deviation of the linear least squares solutions.
[b]Here RS PWV = a × GPS PWV + b.

Table 4. Summary of Comparisons Among RS, GPS, and MODIS PWV in Time Series

Station	Sample Number	*a*	*b*, mm	Standard Deviation, mm[a]	Correlation Coefficient
		GPS PWV Versus RS PWV (Daytime)[b]			
HERS	411	1.02 ± 0.006	−0.3 ± 0.1	0.8	0.99
ARM SGP	263	1.02 ± 0.005	−0.9 ± 0.1	1.2	0.99
		MODIS PWV Versus GPS PWV[c]			
HERS	66	1.09 ± 0.02	−0.3 ± 0.3	1.0	0.97
ARM SGP	21	1.14 ± 0.03	−0.1 ± 0.3	0.8	0.99
		MODIS PWV Versus RS PWV[d]			
HERS	50	1.14 ± 0.03	−0.8 ± 0.5	1.6	0.98
ARM SGP	35	1.20 ± 0.04	−1.4 ± 0.7	2.2	0.96

[a]Standard deviation of the linear least squares solutions.
[b]GPS PWV = a × RS PWV + b.
[c]MODIS PWV = a × GPS PWV + b.
[d]MODISS PWV = a × RS PWV + b.

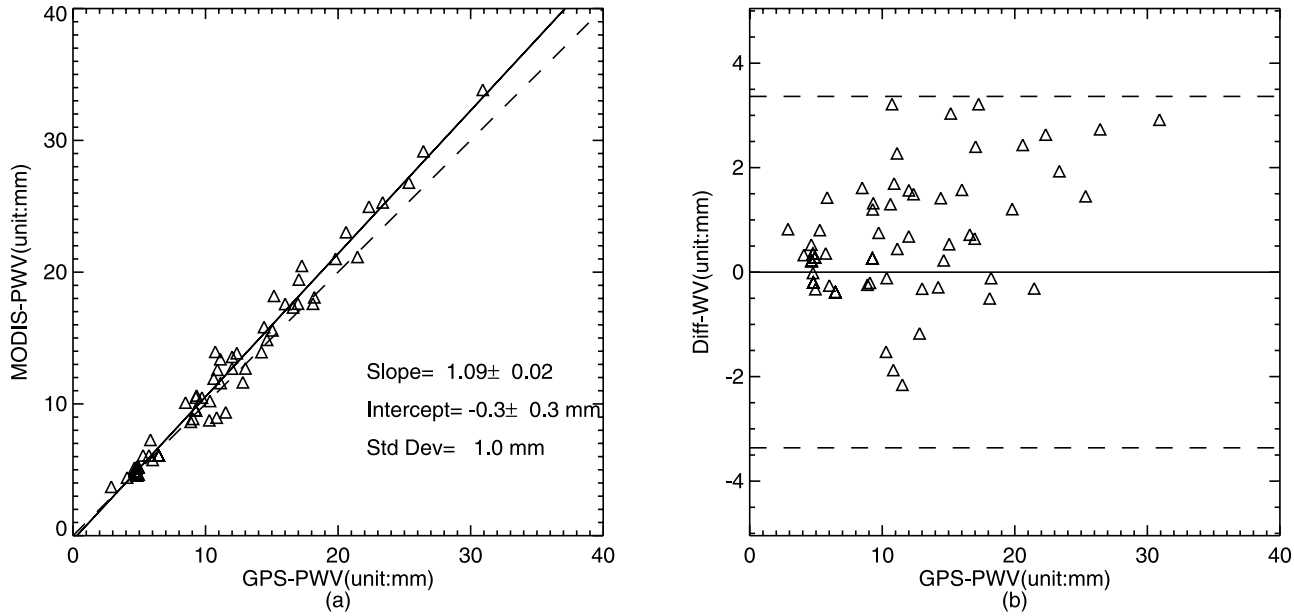

Figure 3. Scatterplots of MODIS PWV and GPS PWV for cloud-free observations at the HERS site from 2 December 2001 to 31 October 2002. (a) The number of valid samples was 66, and 4 samples were omitted due to the 2σ exclusion; (b) difference in PWV (diff-WV) = MODIS PWV − GPS PWV.

deviation of the differences between GPS and RS PWV were 0.1 and 0.8 mm, respectively, at the HERS site and −0.5 and 1.2 mm, respectively, at the ARM SGP site in the daytime. The larger quantity for the ARM SGP site might be attributable to the longer distance between the RS and GPS stations and the larger PWV range.

3.2. Comparisons Between MODIS and GPS PWV

[33] Figure 3a shows the correlation between GPS PWV and MODIS PWV at the HERS station during the period from 2 December 2001 to 31 October 2002. It indicates that MODIS PWV was larger than GPS PWV, with a scale factor of 1.09 ± 0.02. Figure 3b shows that the differences (MODIS PWV - GPS PWV) increased slightly with the amount of PWV. The number of valid pairs was smaller than for the previous comparisons between radiosondes and GPS retrievals because only cloud-free observations were kept and also because there are only two Terra MODIS overpasses a day per location, whereas there can occasionally be up to four radiosonde launches a day as previously mentioned.

[34] The same comparison was performed over 124 GASP GPS stations in Germany. There were at least 10 cloud-free measurements for 86 out of 124 stations. The average scale factor for MODIS PWV with respect to GPS PWV for these 86 stations was 1.07 ± 0.09, with an average offset at zero of −0.8 ± 1.6 mm. Eighteen out of 86 scale factors (21%) were smaller than 1 (i.e., MODIS PWV/GPS PWV < 1), and 68 out of 86 (79%) were greater than 1 (i.e., MODIS PWV/GPS PWV > 1). The average standard deviation of the differences was 1.4 mm.

3.3. Comparisons Between MODIS and RS PWV

[35] As mentioned earlier, radiosondes are usually launched two to four times a day, and MODIS PWV products are only retrieved at most twice a day above one site. Terra MODIS provides a global coverage every 1–2 days and views the Earth's surface near nadir at 1030 LT, so only serendipitous spatiotemporal overlapping data can be found.

[36] Figure 4 shows a comparison of MODIS and RS PWV above the HERS site. The amount of MODIS PWV was 14 ± 3% larger than RS PWV with a zero-point offset of −0.8 ± 0.5 mm. Taking into account the scale factors of GPS PWV relative to RS PWV, MODIS PWV values had a similar linear relationship to RS as to GPS within a 1σ uncertainty. Figure 4b shows clearly that the differences were dependent on the amount of PWV. In other words, the differences (MODIS PWV - RS PWV) increased with the amount of PWV.

4. Spatial Comparisons Between MODIS and GPS PWV

[37] For the first time, a spatial intercomparison of PWV from GPS and MODIS was performed using data collected over Germany (47°–55°N, 6°–15°E) during the period from 1 May 2002 to 30 June 2002. There were 115 Terra overpasses in total in the daytime for this experimental period, with some just over the border of Germany. For each Terra overpass the number of GPS stations with cloud-free conditions varied from 2 to 64 out of 124. A comparison was performed only when at least 10 GPS stations were cloud free. Fifty-nine out of 115 overpasses fulfilled this condition (Table 5). The correlation coefficients between GPS and MODIS PWV for each overpass varied from 0.42 to 0.98, with an average of 0.82. Thirty-six out of 59 scale factors (61%) for MODIS PWV relative to GPS PWV were greater than 1. More importantly, we derived an average linear fit model between MODIS and GPS PWV in this area: MODIS PWV = 1.03(±0.12) × (GPS PWV) − 0.1(±2.3) mm. The average scale factor for this spatial-

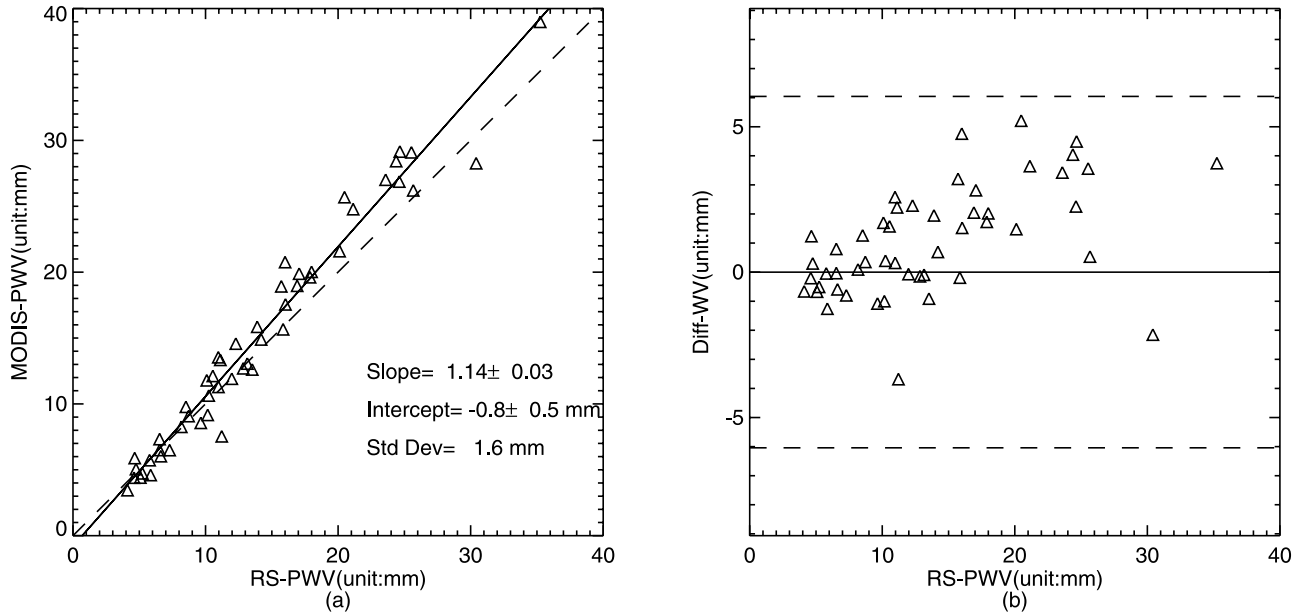

Figure 4. Scatterplots of MODIS PWV and UKMOHF RS PWV for cloud-free observations at the HERS site from 2 December 2001 to 31 October 2002. (a) The number of valid samples was 50, and 2 samples were omitted due to the 2σ exclusion; (b) difference in PWV (diff-WV) = MODIS PWV − RS PWV.

temporal intercomparison was smaller than that in time series (1.07 ± 0.09, cf. section 3.3), but the difference was not significant.

[38] Bearing in mind the good agreements between GPS PWV and MODIS PWV in time series, particularly the small standard deviations of the linear least squares solutions (see Table 4), we used the average linear fit as a model to calibrate MODIS PWV and then compared the calibrated MODIS PWV with GPS PWV (Table 5). After such a correction and 2σ elimination, 58 overpasses fulfilled the requirement that at least 10 GPS stations were cloud free. The average correlation coefficients were almost the same, 0.83 after the correction. However, the average scale factor decreased to 1.01, the average bias from 0.6 to 0.2 mm, and the average standard deviation of the differences from 1.7 to 1.5 mm. Figure 5 shows the distributions of the standard deviations before and after the correction. It indicates that the correction was encouraging, with more standard deviations less than 1 mm and fewer larger than 2 mm after the correction.

5. Discussion

[39] As shown in Table 3, the scale factors of RS and GPS measurements agreed to 4%. In contrast, the scale factors of MODIS PWV varied from 1.09 ± 0.02 to 1.14 ± 0.03 relative to GPS PWV and from 1.14 ± 0.03 to 1.20 ± 0.04 with respect to RS PWV (see section 3.2, Table 4). In other words, GPS PWV and RS PWV agreed better with each other than with MODIS PWV. Figures 2–4 also reveal that the differences relative to MODIS PWV were larger than those between GPS PWV and RS PWV.

[40] The MODIS water vapor amounts are derived from the transmittances based on theoretical calculations and using lookup table procedures. The lookup tables were generated with the HITRAN2000 spectroscopic database

Table 5. Summary of Spatial Comparisons Between MODIS and GPS PWV Across Germany

	Number of Passes	Slope	Intercept, mm	Correlation	Number of Samples	Standard Deviation, mm[a]
Before correction						
Average	59	1.03 ± 0.12	−0.1 ± 2.3	0.82	25	1.7
Minimum	59	0.63 ± 0.41	−8.5 ± 6.0	0.42	10	0.9
Maximum	59	1.44 ± 0.27	8.0 ± 7.9	0.98	69	3.5
After correction						
Average	58	1.01 ± 0.11	−0.1 ± 2.2	0.83	25	1.5
Minimum	58	0.61 ± 0.39	−8.3 ± 5.9	0.34	10	0.8
Maximum	58	1.39 ± 0.26	7.7 ± 7.7	0.98	72	2.8

[a]Standard deviation of differences.

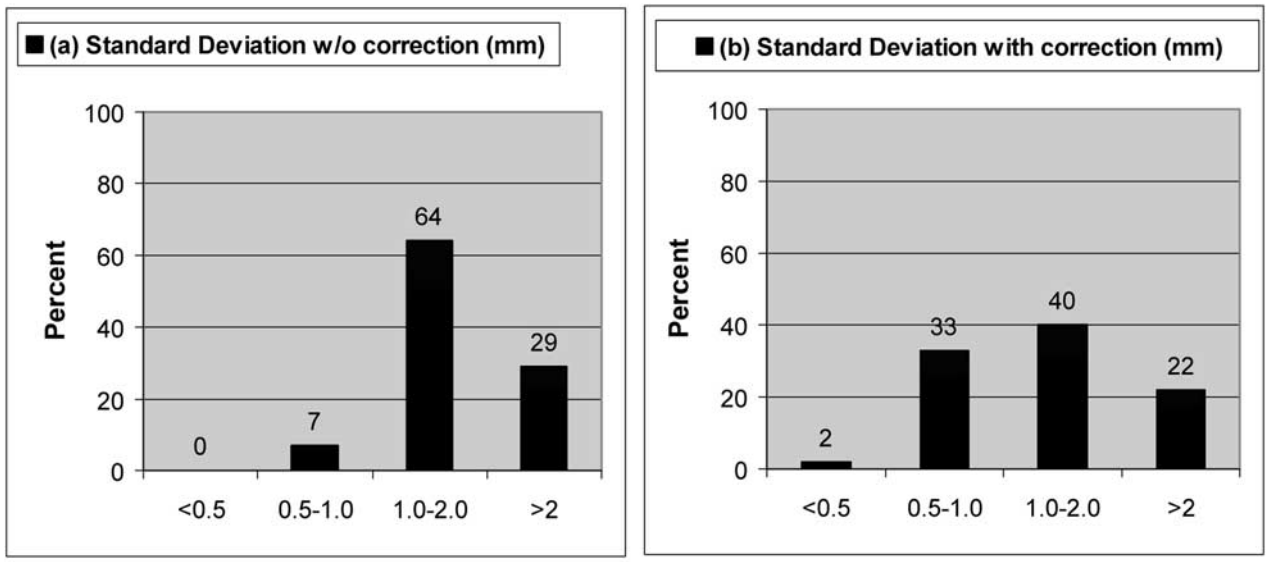

Figure 5. Statistics of spatial comparison between MODIS PWV and GPS PWV throughout Germany during the period from 1 May 2002 to 30 June 2002. (a) Standard deviations of the differences (MODIS PWV − GPS PWV) in millimeters without any correction; (b) standard deviations of the differences (MODIS PWV(calibrated) − GPS PWV) in millimeters after a linear fit model was applied to correct MODIS PWV: MODIS PWV(calibrated) = 1.03 × (MODIS PWV) − 0.1 mm.

and a line-by-line atmospheric transmittance code [*Gao and Kaufman*, 2003]. *Kaufman and Gao* [1992] analyzed the effects of several sources of errors on the MODIS near-IR PWV retrieval: the uncertainty in the spectral reflectance of the surface accounts for 4–7%, haze accounts for 2% or more, sensor calibration accounts for 3–6%, pixel registration between several channels accounts for 2–3%, a shift in channel location accounts for 1–2%, undetected clouds accounts for 1%, atmospheric temperature and moisture profiles account for 1%, and mixed pixels accounts for 0.7%, when additional MODIS channels are utilized. Gao and Kaufman suggested that the presence of haze can result in errors of 10% or slightly greater in the current MODIS water vapor values under hazy conditions (with visibilities less than 10 km) or when the surface reflectances near 1 μm are small (less than about 0.1). Typical errors in the derived water vapor values are estimated to be 5–10% [*Gao and Kaufman*, 2003], and errors can be up to 14% under hazy conditions. As described previously, only MODIS PWV values collected under clear sky conditions were used in this paper. Therefore the MODIS scale uncertainty was considered as 10%. The quadratic sum of the GPS/RS scale uncertainty (4%) and the MODIS typical scale uncertainty (10%) is 11%. The actual scale differences of MODIS/RS are up to 20 ± 4%, which is much larger than the combined uncertainty, suggesting that the MODIS errors are larger than those that can be currently accounted for.

[41] Another possible cause for the larger discrepancies of MODIS PWV relative to GPS/RS could be the different physical principles for the three systems. RS usually take measurements at intervals of approximately 2 s, and measurements were acquired for up to 100 min after launch. Furthermore, RS ZWD is the integration along their flight trajectory, bearing in mind that the horizontal drift of radiosondes might be significant. GPS can take measurements at rates as high as 20 Hz, but CGPS networks typically record data every 30 s; GPS measurements are collected from the whole sky above the cutoff elevation angle (e.g., 5°, 7°, 10°, or 15°). The GPS ZWD was estimated at 5-min intervals (30 min for the GFZ PWV products), so GPS PWV represented a 5-min (or 30-min) average along the paths of 4–12 GPS satellites as they orbited the Earth. In contrast, one scan of the MODIS mirror

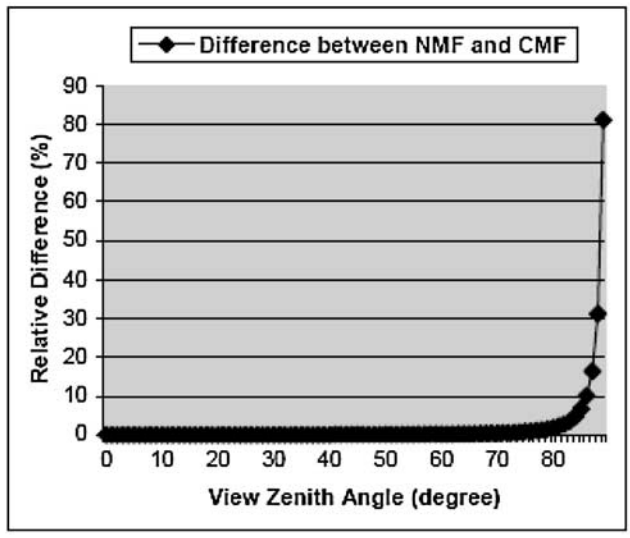

Figure 6. Relative difference between the Cosecant mapping function (CMF) and the Niell Wet mapping function (NMF) at the HERS site at the latitude of 50.9°. The relative difference is 0.3% at 65° view zenith angle and 0.4% at 70°. The accuracy of the CMF with respect to the NMF decreases to 1% at 77°.

takes 1.4771 s to observe a swath (also known as a scan line), which is 2200 km long and 10 km wide at nadir, and MODIS PWV is the instantaneous observation of a 1-km pixel. Furthermore, in this study, the GPS PWV values were averaged over 30-min intervals during the RS launch time when comparing the PWV values derived from GPS with those from RS, but no such averaging was possible when comparing with MODIS.

[42] The adoption of different mapping functions does not contribute significantly to the larger discrepancies of MODIS PWV relative to GPS/RS. The mapping functions, e.g., Niell Mapping Function [*Niell*, 1996], employed for GPS analysis are usually developed on the basis of the radiosonde profiles, which lead to high correlation between GPS and RS ZWD (or PWV). In contrast, a simple Cosecant mapping function (designated CMF) is employed in the processing of MODIS near-infrared water vapor products: $PWV^{*} = PWV(1/\cos\theta + 1/\cos\theta_0)$, where θ is the view zenith angle and θ_0 is the solar zenith angle [*Kaufman and Gao*, 1992]. The view zenith angles vary between $-65°$ and $65°$. The solar zenith angles are typically in the range between $0°$ and $70°$. At high latitudes, the solar zenith angles can be close to $90°$ (B.-C. Gao, private communication, 2003). From Figure 6, the relative difference of CMF with respect to the Niell wet mapping function (designated NMF) is 0.3% at $65°$ view zenith angle and 0.4% at $70°$ at the HERS site. Therefore the difference of the NMF and the CMF could introduce 0.5% error in this study.

[43] In Table 4, the standard deviations of MODIS PWV with respect to RS PWV were larger than those with respect to GPS PWV. This means that MODIS PWV agreed slightly better with GPS PWV than with RS PWV. The different sampling rates and the different observation intervals could be possible explanations. As mentioned above, the difference in the observation intervals between RS and MODIS (i.e., 60–100 min) was much larger than that between GPS and MODIS (i.e., ~5 min).

6. Conclusions

[44] Because of their crucial role in meteorological applications, the potential accuracy of the standard resolution radiosonde data from the UKMO and University of Wyoming (UW) were assessed in this study. The comparisons between high-resolution data and the UKMO and UW standard resolution data showed that some caution needs to be exercised, e.g., missing height values should be filled in when using the UKMO standard resolution data.

[45] Comparisons between the PWV values derived from GPS and radiosonde data were performed. Two types of radiosonde sensors were used in this study. GPS PWV was larger than RS PWV, with a scale factor of 0.96 ± 0.006 at the HERS site for the Vaisala RS80-H radiosondes (Table 3), which is consistent with *Niell et al.*'s [2001] result that the radiosonde PWV scale was ~5% lower than the GPS scale. A significant day-night difference was found only for Vaisala RS90 radiosondes in comparison with GPS PWV, with nighttime launches having a scale factor 4% larger, but agreeing overall better.

[46] In this study, the MODIS PWV Collection 3 products were evaluated using radiosondes and GPS. In order to be consistent with the other two data sets, only the daytime radiosonde measurements were used in the comparisons. MODIS PWV overestimated PWV against radiosondes, with scale factors from 1.14 to 1.20, and the standard deviations ranged from 1.6 to 2.2 mm. MODIS PWV overestimated PWV against GPS by a factor from 7 to 14%, with standard deviations varying from 0.8 to 1.4 mm in time series. For the first time, MODIS PWV was compared with GPS PWV spatially using the GASP GPS network in Germany. Taking into account the good linear relationship between MODIS PWV and GPS PWV in time series, we derived an average linear fit model in this area and applied this model to calibrate MODIS PWV values. The calibrated MODIS PWV appeared to be in closer agreement with GPS PWV, having smaller offsets, a slope closer to unity, smaller biases, and smaller standard deviations. The correction method is worth investigating further, and the coefficients could be updated as a function of location for a given period of time.

[47] Taking into account the large scale factors of MODIS PWV relative to RS PWV and GPS PWV, it is recommended that the MODIS water vapor products should be updated or calibrated (e.g., using a linear model as proposed above) before being applied to correct InSAR atmospheric effects.

[48] The Medium-Resolution Imaging Spectrometer (MERIS) was launched together with the advanced synthetic aperture radar (ASAR) on the ESA ENVISAT spacecraft on 1 March 2002. Although MERIS and ASAR are operated independently, these data can be acquired simultaneously during daytime. MERIS produces precipitable water vapor products with a better spatial resolution (300 m compared with 1 km for MODIS), and the accuracy of MERIS precipitable water vapor products is expected to be higher than MODIS PWV (J. Fischer, private communication, 2002). As with MODIS PWV, the limitations in MERIS precipitable water vapor products will be their limited operating time (i.e., only daytime) and the requirement for cloud-free conditions. The latter restricts the regular applications of MERIS precipitable water vapor products to arid areas or midlatitude/high-latitude areas primarily in the winter season.

[49] In the near future, MERIS precipitable water vapor products will be evaluated using RS and GPS measurements, and methods to integrate MERIS precipitable water vapor and GPS PWV will be explored. Our main application will be to correct InSAR measurements using GPS and MERIS precipitable water vapor products.

[50] **Acknowledgments.** This research is supported by Overseas Research Students Awards (ORS) and UCL Graduate School Research Scholarships at University College London. This work is also supported by the NERC Earth Observation Centre of Excellence: Centre for the Observation and Modelling of Earthquakes and Tectonics (COMET). We thank A. Niell and V. Mendes for providing us with the ray-tracing program. We would also like to express our appreciation to Christoph Reigber, Gerd Gendt, and Yanxiong Liu for providing us with GFZ PWV products, to Paul Odams and Jonathan Jones of the UK Met Office for providing us with high-resolution radiosonde data for the Herstmonceux station, and to Eugene Clothiaux of Penn State University for providing us with high-resolution radiosonde data for the ARM SGP station. We appreciate the useful discussions with Catherine Naud and the extremely valuable suggestions of the two anonymous referees, both of whom have put a considerable amount of time and effort into reviewing and improving this paper. The standard radiosonde data are courtesy of the British Atmospheric Data Centre (BADC, http://badc.nerc.ac.uk/home/) and University of Wyoming (http://weather.uwyo.edu/upperair/sounding.html). The MODIS

water vapor data, classified as "validated products," were obtained from the Goddard Earth Sciences Distributed Active Archive Center (DAAC) and the GPS data were obtained from Scripps Orbit and Permanent Array Centre (SOPAC, http://sopac.ucsd.edu/).

References

American Meteorological Society (AMS), *Glossary of Meteorology*, 2nd ed., Boston, Mass., 2000.

Bar-Sever, Y. E., and P. M. Kroger, Strategies for GPS-based estimates of troposphere delay, paper presented at 9th International Technical Meeting of the Satellite Division of the U.S. Institute of Navigation (GPS ION-96), Kansas, Mo., 17–20 Sept. 1996.

Bevis, M., S. Businger, T. A. Herring, C. Rocken, R. A. Anthes, and R. H. Ware, GPS meteorology: Remote sensing of atmospheric water vapor using the Global Positioning System, *J. Geophys. Res.*, *97*, 15,787–15,801, 1992.

Bevis, M., S. Businger, S. Chiswell, T. Herring, R. Anthes, C. Rocken, and R. Ware, GPS meteorology: Mapping zenith wet delays onto precipitable water, *J. Appl. Meteorol.*, *33*, 379–386, 1994.

Chaboureau, J. P., A. Chédin, and N. A. Scott, Remote sensing of the vertical distribution of the atmospheric water vapor from the TOVS observations: Method and validation, *J. Geophys. Res.*, *103*, 8743–8752, 1998.

Davis, J. L., T. A. Herring, I. I. Shapiro, A. E. E. Rogers, and G. Elgered, Geodesy by radio interferometry: Effects of atmospheric modeling errors on the estimates of the baseline length, *Radio Sci.*, *20*(6), 1593–1609, 1985.

Emardson, T. R., G. Elgered, and J. M. Johansson, Three months of continuous monitoring of atmospheric water vapor with a network of Global Positioning System receivers, *J. Geophys. Res.*, *103*, 1807–1820, 1998.

Emardson, T. R., J. Johansson, and G. Elgered, The systematic behavior of water vapor estimates using four years of GPS observations, *IEEE Trans. Geosci. Remote Sens.*, *38*(1), 324–329, 2000.

Ferrare, R., L. Brasseur, M. Clayton, D. Turner, L. Remer, and B. C. Gao, Evaluation of TERRA aerosol and water vapor measurements using ARM SGP data, paper presented at American Meteorological Society 11th Conference on Atmospheric Radiation, Ogden, Utah, 3–7 June 2002.

Gao, B.-C., and Y. J. Kaufman, Water vapor retrievals using Moderate Resolution Imaging Spectroradiometer (MODIS) near-infrared channels, *J. Geophys. Res.*, *108*(D13), 4389, doi:10.1029/2002JD003023, 2003.

Gendt, G., C. Reigber, and G. Dick, Near real-time water vapor estimation in a German GPS network: First results from the ground program of the HGF GASP project, *Phys. Chem. Earth, Part A*, *26*(6–8), 413–416, 2001.

Hanssen, R. F., A. J. Feijt, and R. Klees, Comparison of precipitable water vapor observations by spaceborne radar interferometry and Meteosat 6.7 μm radiometry, *J. Atmos. Oceanic Technol.*, *18*, 756–764, 2001.

Kaufman, Y. J., and B. Gao, Remote sensing of water vapor in the near IP from EOS/MODIS, *IEEE Trans. Geosci. Remote Sens.*, *30*(5), 871–884, 1992.

Liljegren, J., B. Lesht, T. VanHove, and C. Rocken, A comparison of integrated water vapor from microwave radiometer, balloon-borne sounding system, and Global Positioning System, paper presented at 9th ARM Science Team Meeting, San Antonio, Tex., 22–26 March 1999.

MacMillan, D. S., and C. Ma, Evaluation of very long baseline interferometry atmospheric modeling improvements, *J. Geophys. Res.*, *99*, 637–651, 1994.

Mendes, V. B., G. Prates, L. Santos, and R. B. Langley, An evaluation of models for the determination of the weighted mean temperature of the atmosphere, paper presented at Institute of Navigation 2000 National Technical Meeting, Anaheim, Calif., 26–28 Jan. 2000.

Mockler, S. B., Water vapor in the climate system, special report, AGU, Washington, D. C., Dec. 1995.

Niell, A. E., Global mapping functions for the atmospheric delay at radio wavelengths, *J. Geophys. Res.*, *101*, 3227–3246, 1996.

Niell, A. E., A. J. Coster, F. S. Solheim, V. B. Mendes, P. C. Toor, R. B. Langley, and C. A. Upham, Comparison of measurements of atmospheric wet delay by radiosonde, water vapor radiometer, GPS, and VLBI, *J. Atmos. Oceanic Technol.*, *18*, 830–850, 2001.

Quinn, K. J., and T. A. Herring, GPS atmospheric water vapor measurements without surface pressure sensors, *Eos Trans. AGU*, *77*(46), Fall Meet. Suppl., F134, 1996.

Randel, D. L., T. J. Greenwald, T. H. V. Haar, G. L. Stephens, M. A. Ringerud, and C. L. Combs, A new global water vapor dataset, *Bull. Am. Meteorol. Soc.*, *77*(6), 1233–1254, 1996.

Reigber, C., G. Gendt, G. Dick, and M. Tomassini, Near-real-time water vapor monitoring for weather forecasts, *GPS World*, *13*(1), 18–27, 2002.

Rocken, C., T. V. Hove, and R. Ware, Near real-time GPS sensing of atmospheric water vapor, *Geophys. Res. Lett.*, *24*(24), 3221–3224, 1997.

Smout, S., J. Elms, D. Lyth, and J. Nash, Met Office RS90 humidity sensor evaluations, Met Off., Berkshire, UK, 2001.

Wang, J. H., Understanding and correcting humidity measurement errors from Vaisala RS80 and VIZ radiosondes, paper presented at Radiosonde Workshop, Hampton Univ., Hampton, Va., 21–23 May 2002.

Wang, J. H., H. L. Cole, D. J. Carlson, E. R. Miller, K. Beierle, A. Paukkunen, and T. K. Laine, Corrections of humidity measurement errors from the Vaisala RS80 radiosonde: Application to TOGA COARE data, *J. Atmos. Oceanic Technol.*, *19*, 981–1002, 2002.

Williams, S., Y. Bock, and P. Fang, Integrated satellite interferometry: Troposphere noise, GPS estimates, and implications for synthetic aperture radar products, *J. Geophys. Res.*, *103*, 27,051–27,067, 1998.

Wright, J., Rawinsonde and pibal observations, *Fed. Meteorol. Handb. 3, FCM-H3-1997*, Off. of the Fed. Coord. for Meteorol., Washington, D. C., May 1997.

Zebker, H. A., P. A. Rosen, and S. Hensley, Atmospheric effects in interferometric synthetic aperture radar surface deformation and topographic maps, *J. Geophys. Res.*, *102*, 7547–7563, 1997.

Zumberge, J. F., M. B. Heflin, D. C. Jefferson, and M. M. Watkins, Precise point positioning for the efficient and robust analysis of GPS data from large networks, *J. Geophys. Res.*, *102*, 5005–5017, 1997.

P. Cross, Z. Li, and J.-P. Muller, Department of Geomatic Engineering, University College London, Gower Street, London, WC1E 6BT, UK. (zhli@ge.ucl.ac.uk)